ELSEVIER

Journal of Nuclear Materials 307–311 (2002) 918–923

journal of nuclear materials

www.elsevier.com/locate/jnucmat

Growth and instability of charged dislocation loops under irradiation in ceramic materials

A.I. Ryazanov [a,*], K. Yasuda [b], C. Kinoshita [b], A.V. Klaptsov [a]

[a] *Institute of General and Nuclear Physics, Russian Research Centre Kurchatov Institute, 123182 Moscow, Russia*
[b] *Department of Applied Quantum Physics and Nuclear Engineering, Kyushu University, Fukuoka 812-8581, Japan*

Abstract

We have investigated the physical mechanisms of the growth and stability of charged dislocation loops in ceramic materials with very strong different mass of atoms (stabilized cubic zirconia) under different energies and types of irradiation conditions: 100–1000 keV electrons, 100 keV He^+ and 300 keV O^+ ions. The anomalous formation of extended defect clusters (charged dislocation loops) has been observed by TEM under electron irradiation subsequent to ion irradiation. It is demonstrated that very strong strain field (contrast) near charged dislocation loops is formed. The dislocation loops grow up to a critical size and after then become unstable. The instability of the charged dislocation loop leads to the multiplication of dislocation loops and the formation of dislocation network near the charged dislocation loops. A theoretical model is suggested for the explanation of the growth and stability of the charged dislocation loop, taking the charge state of point defects. The calculated distribution of the modified strain field by the electrical field around the charged dislocation loops is stronger than that of noncharged dislocation loops. The obtained theoretical results for the modified strain field contrast and the critical radius of unstable charged dislocation loops are compared with observed experimental data.

1. Introduction

Ceramic materials have potentials to be applied in future fusion reactors as radio frequency windows, toroidal insulating breaks and diagnostic probes. The radiation resistance of those materials is determined by the kinetics of radiation-induced point defects and point defect cluster formation (dislocation loops, voids etc.). Under ionizing radiation process, the excitation of the electronic subsystem and the covalent type of interaction between lattice atoms and point defects in ceramic materials are characterized by the effective charge. The different production rate of point defects of constituent atoms due to different mass and displacement energies is also an important character in multi-component ceramic materials.

In the present paper, we have investigated the physical mechanisms of strain and stress contrast formation near charged dislocation loops in stabilized cubic zirconia whose mass of constituent ions is remarkably different. Previous studies [1–3] have shown that this material is exceptionally radiation resistant, especially to amorphization and radiation swelling. The anomalous formation of extended defect clusters (charged dislocation loops) has been observed using microstructure investigations by TEM under electron irradiation subsequent to ion irradiation. The characteristics of defect clusters will be shown with emphasis on the strong strain field and the instability of the defects. A theoretical model and numerical calculations of strain and stress contrast formation near charged dislocation loops are also presented, taking into account the charge state of point defects in dislocation loops and the effect of electric and elastic fields on strain and stress distribution.

* Corresponding author. Tel.: +7-095 196 91 77; fax: +7-095 421 45 98.
E-mail address: ryazanoff@comail.ru (A.I. Ryazanov).

0022-3115/02/$ - see front matter
PII: S0022-3115(02)01122-4

2. Experimental results

Single crystals of 13 mol% yttrium stabilized cubic zirconia (ZrO_2–$13Y_2O_3$: YSZ, Earth Jewelry Co.) were used in this experimental study. Thin foil specimens whose surfaces are close to {1 1 1} planes were prepared for electron transparency by using the ion-thinning technique with 4 keV Ar^+ ions. The specimens were annealed in air at 1670 K to remove radiation defects induced by the ion-thinning process. The thin foil specimens were irradiated with 100 keV He^+ ions at 870 K or with 300 keV O^+ ions at 470 K. Following the ion irradiation, the specimens were subjected to electron irradiation with energies from 100 to 1000 keV at 370–870 K. The microstructure evolution was recorded during or after irradiation either on films or video tapes. The irradiation and TEM investigations were performed at the HVEM Laboratory, Kyushu University and TIARA of JAERI.

Irradiation with 300 keV O^+ ions to 2 dpa and with 100 keV He^+ ions to 0.6 dpa results in tiny dot contrast features. In contrast, the subsequent electron irradiation performed after those ion irradiation has shown the production of large extended defects. Fig. 1 shows the typical microstructure showing such defect clusters obtained by the subsequent electron irradiation with 400 keV after 300 keV O^+ ion irradiation. These defect clusters have the average diameter of around 500 nm. The main peculiarity of these extended defects is that they exhibit strong black/black lobes contrast, indicating that there exists a very strong strain field around the defect clusters. The second important point is that the defects are formed preferentially around the focused electron beam. It suggests that a flow of point defects due to the flux distribution of the focused electron beam plays an important role for the nucleation of defect clusters. Furthermore, bright-field images of the defect clusters with three different 220 diffraction vectors, using a [1 1 1] incident electron beam, have revealed a similar black/black lobes contrast (as an example is shown in Fig. 2(a)) but showed no contrast lines perpendicular to each 220 diffraction vector [4]. This clearly indicates that the defect clusters possess an isotropic strain field on the (1 1 1) plane and are not typical perfect dislocation loops.

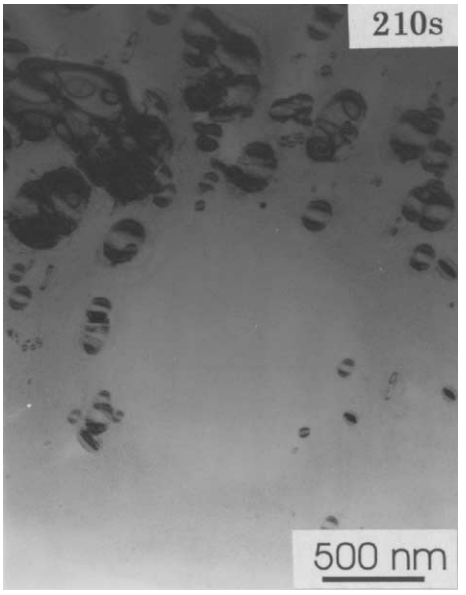

Fig. 1. Bright-field micrograph of YSZ irradiated with 400 keV electrons at 470 K following 300 keV O^+-ion irradiation at 470 K to a fluence of 5.1×10^{17} O^+/m^2.

A very interesting process is the growth kinetics of the defect clusters under electron irradiation. Fig. 2 demonstrates a sequence of the growth process of the defect cluster under 200 keV electron irradiation at 470 K. The strain contrast around the defect cluster is seen to increase with electron irradiation. It means that the growth stage is characterized by the increasing of the elastic strain around the cluster. At the critical size of about 1.2 μm the strong double-arc contrast disappears and it is suddenly converted to contrast for normal dislocation lines. It is a completely new phenomenon related to the multiplication of dislocations in ceramic materials under irradiation. For the explanation of this phenomenon the following theoretical model is suggested.

3. Theoretical model

The microstructure change and point defect cluster formation in cubic zirconia under electron irradiation are determined by generation rates of point defects in two subsystems: Zr and O atoms. The main part of point defects produced under electron irradiation of cubic zirconia in the energy interval from $E_e = 100$ keV to $E_e = 1$ MeV are oxygen point defects (interstitials and vacancies). This is due to the strong difference of the mass of atoms and displacement energies of the Zr and O atoms. Indeed, for lighter oxygen atoms the displacement energy of oxygen E_d^O is less compared with zirconium E_d^{Zr} ($E_d^O = 20$ eV and $E_d^{Zr} = 40$ eV), and at low irradiation electron energy especially at $E_e = 100$ keV only oxygen atoms will be displaced. The displacement cross-section for oxygen atoms σ_d^O due to the elastic collisions of fast electrons with target atoms is much higher compared with zirconium atoms σ_d^{Zr} ($\sigma_d^O \gg \sigma_d^{Zr}$). (So for the comparison at energies $E_e = 1.09$ MeV, $\sigma_d^O = 36$ barn and at $E_e = 1.03$ MeV, $\sigma_d^{Zr} = 4.23$ barn [5].) Such displaced interstitial oxygen atoms in cubic zirconia have the effective charge (O^{-2}) [6]. These effective charges of interstitial oxygen atoms and vacancies are

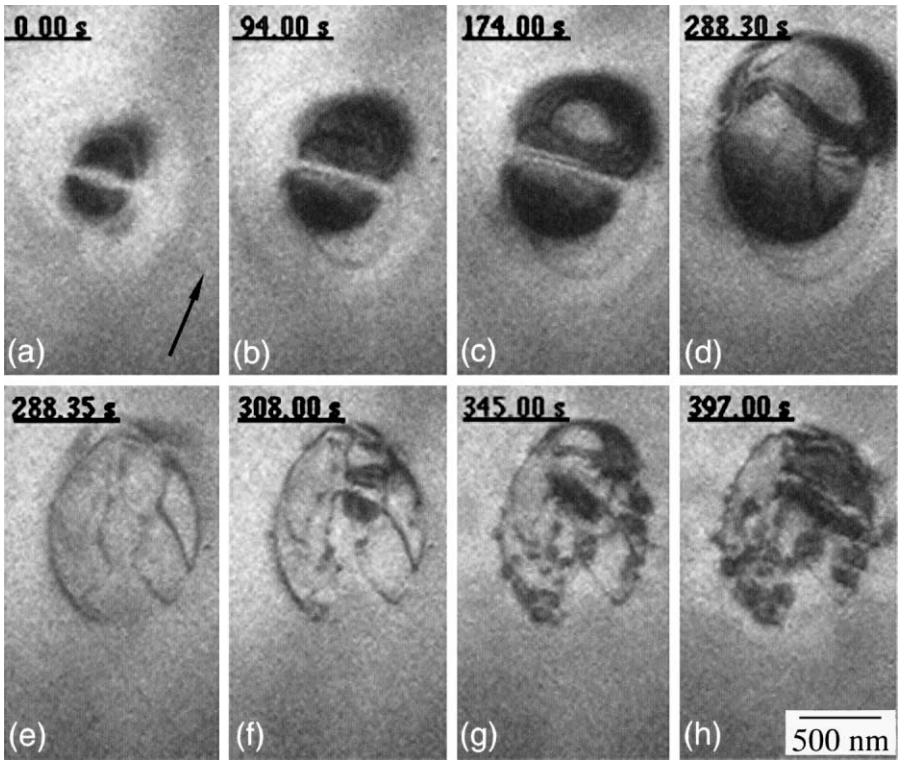

Fig. 2. The growth of defect clusters shown in Fig. 1 under 200 keV electron irradiation at 470 K. The samples were irradiated originally with 300 keV O^+ ions at 470 K to a fluence of 5.1×10^{17} O^+/m^2. Irradiation time from the upper-left micrograph is also shown at each micrograph.

determined by the kinetics of emission and absorption of electrons on these point defects [7]. We will assume that each interstitial oxygen atom during the diffusion process has the same effective charge (O^{-2}) in the present study. The energy migration barrier for interstitial oxygen atoms is less compared with that for interstitial zirconium atoms. This means that due to the high diffusivity and agglomeration of charged interstitial oxygen atoms in the matrix, the clusters of charged oxygen interstitial atoms (charged interstitial dislocation loops) can be formed. The atomistic configurations of such dislocation loop core is not yet clear.

As already mentioned in Section 2, a strong double contrast near the defect clusters exists in stabilized cubic zirconia. This double contrast is determined by the distribution of strong stress and strain fields near such clusters. The charged dislocation loop or platelet will produce in the matrix an addition mechanical stress field with the stress tensor σ_{ch}. The shape and nature of stress and strain fields near charged dislocation loops are completely different compared with normal dislocation loops. Let us calculate and compare the distribution stress and strain fields for charged and normal (non-charged) dislocation loops.

The charged dislocation loops produce in the matrix an electrical field ($\boldsymbol{E}$) which is determined by the distribution of the electrical potential (ϕ) near the charged dislocation loop ($\boldsymbol{E} = -\nabla\phi$) defined by the Poisson equation:

$$\Delta\phi = 0. \tag{1}$$

The solution of this equation near a circular charged dislocation loop with the radius $R(R \gg b)$ in cylindrical geometry can be rewritten in the following form:

$$\phi(\rho, z) = \frac{qb}{\omega\zeta} \int_0^{2\pi} \mathrm{d}\varphi' \int_0^R \frac{\rho' \,\mathrm{d}\rho'}{[z^2 + \rho^2 + \rho'^2 - 2\rho\rho' \cos\varphi']^{1/2}}. \tag{2}$$

Here b is the Burgers vector of the charged dislocation loop, ζ is the dielectric permeability of material, q is the effective charge of atoms in dislocation loop; ρ, z, φ are the cylindrical coordinates $(z^2 + \rho^2 = r^2, \rho = r\sin\vartheta)$. Using the new variables,

$$k^2 = \frac{4\chi\Re\sin\vartheta}{\Re^2 + \chi^2 + 2\chi\Re\sin\vartheta}, \quad \chi = \frac{\rho'}{R}, \quad \Re = \frac{r}{R},$$

we can rewrite Eq. (2) in the following form:

$$\phi(r) = \frac{4qbR}{\omega\zeta} \int_0^1 \frac{\chi \, d\chi}{(\Re^2 + \chi^2 + 2\chi\Re \sin\vartheta)^{1/2}} K(k),$$

$$K(k) = \int_0^{\pi/2} \frac{d\beta}{\sqrt{1 - k^2 \sin^2 \beta}}. \quad (3)$$

The electrical field $\boldsymbol{E}$ in ceramic (dielectric) materials produces near the circular charged dislocation loop an additional stress field σ_{ik}^{E}, which is given by the following relation [8],

$$\sigma_{ik}^{E} = \frac{\zeta}{4\pi}\left(E_i E_k - \frac{E^2}{2}\delta_{ik}\right). \quad (4)$$

Here ζ is the dielectric constant (permeability), δ_{ik} is the Kronecker's delta function.

The shear (σ_{zr}) and normal (σ_{zz}) components of the stress tensor (4) produced by the electrical field have been calculated here. The elastic stress field and the components of the stress tensor σ_{ik}^{Y} near a pure (noncharged) prismatic dislocation loop which is located in the (x, y) plane with the Burgers vector $b(0, 0, b)$ is well known from the dislocation theory [9,10]. The total stress field near a charged dislocation loop (σ_{ik}) is determined by the sum of the normal elastic stress field (σ_{ik}^{Y}) and an additional stress field induced by the electrical field near the dislocation loop (σ_{ik}^{E}),

$$\sigma_{ik} = \sigma_{ik}^{Y} + \sigma_{ik}^{E}. \quad (5)$$

The numerical calculations of the total stress field (5) near the charged dislocation loop taking into account the induced stress field by the electrical field and the usual elastic stress field give the stress tensor components which are shown in Figs. 3 and 4.

The components of the strain tensor ε_{ik} can be found from Hooke's law,

$$\sigma_{ik} = \lambda\varepsilon_{ll}\delta_{ik} + 2\mu\varepsilon_{ik}. \quad (6)$$

We can see that the total strain field (ε_{ik}) in the linear elastic theory is also equal to the sum of the usual elastic strain field (ε_{ik}^{Y}) and the additional strain field produced by the electrical field (ε_{ik}^{E}). The numerical calculations of the total strain ε_{zz}^{tot} formed near charged dislocation loop are presented in Fig. 5. The following constants are used for the numerical calculations for cubic zirconia [11]: $\mu = C_{44} = 60$ GPa, $\lambda = C_{12} = 100$ GPa, $v = 0.3$, $b = 0.51$ nm, $q = -2e$; (q is the effective charge per one oxygen atom (interstitial) in the dislocation loop, $e = 4.8 \times 10^{-10}$, e is the electron charge), $R = Nb$ ($N = 300$, $R = 1500$ A, $\rho = 6$ (g/cm^3), $\zeta = 12.5$ (ζ is the dielectric permeability of ZrO_2) [12].

The numerical calculations show that the distribution of the modified strain field by the electrical field near charged dislocation loops is much stronger compared with noncharged dislocation loops and it is determined completely by the electrical field (see Fig. 5).

The critical conditions for the multiplication of dislocations (new dislocation loop punching) near the charged dislocation loop is determined by the conditions for the beginning of plastic deformation. This process is

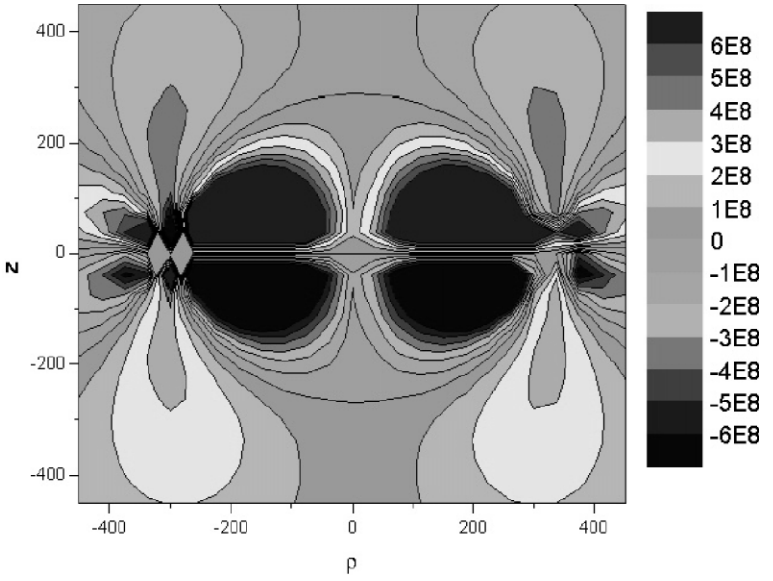

Fig. 3. Distribution of the total shear stress tensor component $(\sigma_{z\rho}^{tot})$ near a charged dislocation loop with radius $R = 150$ nm (σ is in dyn/cm^2).

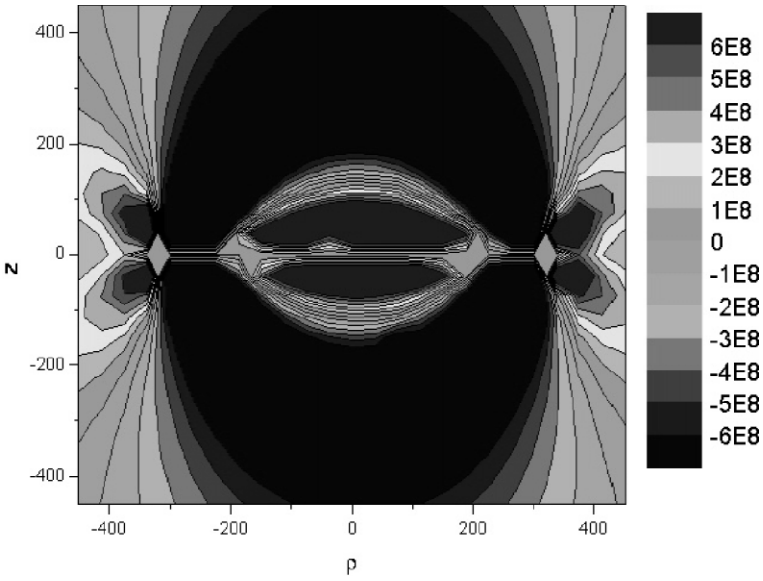

Fig. 4. Distribution of the total normal stress tensor component ($\sigma_{zz}^{\mathrm{tot}}$) near a charged dislocation loop with radius $R = 150$ nm (σ is in dyn/cm^2).

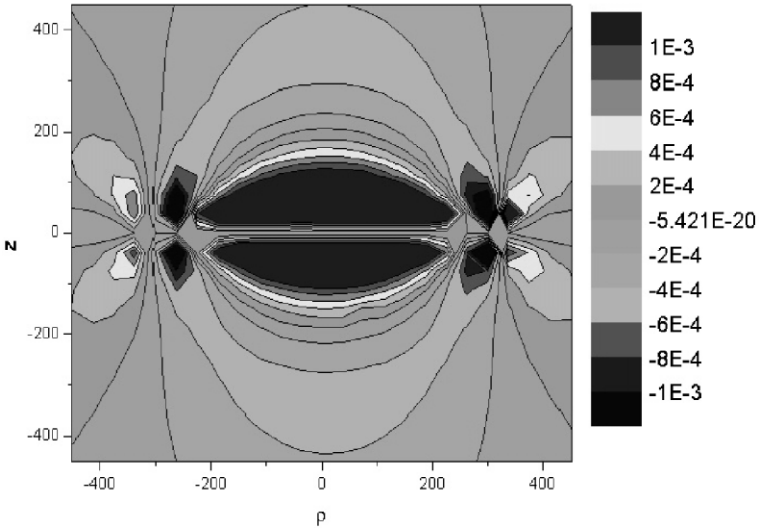

Fig. 5. Distribution of the total strain tensor component ($\varepsilon_{zz}^{\mathrm{tot}}$) produced by electrical field near a charged dislocation loop with radius $R = 1500$ A.

started when the maximum value for the shear stress tensor component (5) exceeds the yield stress (σ_{Y}),

$$\sigma_{ik} = \sigma_{\mathrm{Y}}. \tag{7}$$

The theoretical value of shear strength is equal to $\sigma_{\mathrm{Y}}^{\mathrm{th}} = \mu/2\pi \approx 10^{-1}\mu$ [9]. The real experimental value of the yield stress is less than the theoretical value and is expressed as $\sigma_{\mathrm{Y}} \approx 10^{-2}$–$10^{-3}\mu$ [9]. We have used the experimental value of yield stress $\sigma_{\mathrm{Y}} = 10^{-3}\ \mu$ in our calculations for getting a physical picture of this phenomenon. However, it should be remarked here that because the electrical potential near charged dislocation loop $\phi \propto R^2$ (see (3)) and $\sigma_{ik}^{\mathrm{E}} \propto E^2 \propto (\mathrm{grad}\,\varphi)^2 \propto R^4$ for large dislocation loops, the theoretical shear strength $\sigma_{\mathrm{Y}}^{\mathrm{th}}$ may be exceeded too. The critical radius (R_{cr}) for the beginning of multiplication of near charged dislocation loops can be found from the following relation,

$$\sigma_{ik}(R_{\mathrm{cr}}) = \sigma_{\mathrm{Y}} \tag{8}$$

and the critical radius R_{cr} is proportional to $(\sigma_Y)^{1/4}$ because $\sigma_{ik}^E \propto R^4$. The brown areas in Figs. 3 and 4 show the regions where the plastic deformation can start ($\sigma \geqslant \sigma_Y \approx 10^9$ dyn/cm^2). From the obtained numerical calculations we can see that the total stress (shear and normal components of the stress tensor) near charged dislocation loop can exceed the yield stress (in the brown regions of these figures) and plastic deformation (multiplication of new dislocation loops) can start here.

4. Conclusions

Based on the experimental and theoretical results presented in this paper we can make the following conclusions:

1. Electron-irradiation subsequent to ion-irradiation induces anomalous large defect clusters with strong stress and strain fields in yttria-stabilized cubic zirconia (YSZ).
2. Such defect clusters are considered to be oxygen charged clusters, which are formed due to the production of displacement oxygen atoms in multi-component ZrO_2–Y_2O_3 ceramics.
3. Under irradiation, the growth of charged defect clusters can result in the multiplication of the dislocations in fusion ceramics due to the beginning of plastic deformation in the strong stress and strain fields near such defect clusters.

References

[1] K. Yasuda, C. Kinoshita, T. Inoue, S. Matsumura, H. Abe, K.E. Sickafus, JAERI Rev. 99-025 (1999) 149.
[2] K. Yasuda, M. Nastasi, K.E. Sickafus, et al., Nucl. Instrum. and Meth. B 136–138 (1998) 499.
[3] K.E. Sickafus, Hj. Matzke, K. Yasuda, et al., Nucl. Instrum. and Meth. B 141 (1998) 358.
[4] K. Yasuda, C. Kinoshita, in preparation.
[5] O.S. Oen, Cross sections for atomic displacements in solids by fast electrons, ORNL-4897 (1973).
[6] S.J. Zinkle, C. Kinoshita, J. Nucl. Mater. 251 (1997) 200.
[7] A.I. Ryazanov, C. Kinoshita, Nucl. Instrum. and Meth. B, in press.
[8] L.D. Landau, E.M. Lifshitz, Electrodynamic of Continuous Media, Moscow, 1959.
[9] J.R. Hirth, J. Lothe, Theory of Dislocations, New York, 1968.
[10] F. Kroupa, Theory of crystal defects, in: Proceedings of the Summer School held in Hrazany in September 1964, p. 275.
[11] H.M. Kandil, J.D. Greiner, J.F. Smith, J. Amer. Ceram. Soc. 67 (1984) 341.
[12] D.R. Lide, Handbook of Chemistry and Physics, 80th edition, CRC Press, New York, 1999.